THE JOURNAL OF BIOLOGICAL CHEMISTRY VOL. 289, NO. 17, pp. 11695–11703, April 25, 2014

Differential Transmembrane Domain G*XXX*G Motif Pairing Impacts Major Histocompatibility Complex (MHC) Class II Structure*

Received for publication, September 9, 2013, and in revised form, March 9, 2014 Published, JBC Papers in Press, March 11, 2014, DOI 10.1074/jbc.M113.516997

Ann M. Dixon[‡], Lisa Drake[§], Kelly T. Hughes[§], Elizabeth Sargent[§], Danielle Hunt[§], Jonathan A. Harton[§], and James R. Drake[§1]

From the [‡]Department of Chemistry, University of Warwick, Coventry CV4 7AL, United Kingdom and the [§]Center for Immunology and Microbial Disease, Albany Medical College, Albany, New York 12208

Background: Major histocompatibility complex class II molecules are structurally and functionally heterogeneous.
Results: Combined mutagenesis and structural studies establish a role for pairing between conserved transmembrane (TM) G*XXX*G dimerization motifs in determining class II conformation.
Conclusion: Differential pairing of highly conserved TM domain dimerization motifs contributes to class II structure and function.
Significance: Global conformation contributes to the function of peptide-class II complexes.

Major histocompatibility complex (MHC) class II molecules exhibit conformational heterogeneity, which influences their ability to stimulate CD4 T cells and drive immune responses. Previous studies suggest a role for the transmembrane domain of the class II $\alpha\beta$ heterodimer in determining molecular structure and function. Our previous studies identified an MHC class II conformer that is marked by the Ia.2 epitope. These Ia.2$^+$ class II conformers are lipid raft-associated and able to drive both tyrosine kinase signaling and efficient antigen presentation to CD4 T cells. Here, we establish that the Ia.2$^+$ I-A^k conformer is formed early in the class II biosynthetic pathway and that differential pairing of highly conserved transmembrane domain G*XXX*G dimerization motifs is responsible for formation of Ia.2$^+$ *versus* Ia.2$^-$ I-A^k class II conformers and controlling lipid raft partitioning. These findings provide a molecular explanation for the formation of two distinct MHC class II conformers that differ in their inherent ability to signal and drive robust T cell activation, providing new insight into the role of MHC class II in regulating antigen-presenting cell-T cell interactions critical to the initiation and control of multiple aspects of the immune response.

Major histocompatibility complex (MHC) class II-restricted antigen presentation by B cells, macrophages, and dendritic cells is central to the recruitment and activation of CD4$^+$ T cells. Class II-restricted antigen presentation by B cells to effector CD4 T cells is especially critical for the formation of extrafollicular antibody-producing cells as well as the formation and maturation of germinal centers (1).

MHC class II molecules are $\alpha\beta$ heterodimers that assemble in the endoplasmic reticulum (ER)[2] under the guidance of a third protein, invariant chain (Ii, CD74). Nonameric class II-Ii complexes exit the ER and are delivered to an endocytic compartment where Ii is proteolytically degraded and stripped from class II by the action of the MHC class II-like chaperone DM. DM also facilitates binding of antigenic peptide (derived from the proteolytic processing of exogenous antigen) and then releases resulting peptide-class II complexes for delivery to the cell surface.

Multiple lines of evidence suggest that MHC class II molecules exist in more than one conformational state. Identification of SDS-stable *versus* unstable peptide-class II complexes suggested that class II molecules could exist in at least two different conformational states, in this case driven primarily by the properties of the bound peptide (2, 3). Identification of "Type A" and "Type B" T cells further suggests the existence of distinct forms of peptide-class II complexes, the formation of which is highly dependent on the mechanism of MHC class II peptide loading (4). Most recently, we identified a subset of signaling-competent lipid raft-tropic I-A^k class II molecules bearing the Ia.2 epitope, which is recognized by the 11-5.2 anti-Ia.2 mAb. We demonstrated that these Ia.2$^+$ class II molecules are more efficient at stimulating T cells than Ia.2$^-$ peptide-class II complexes (5). When analyzed by SDS-PAGE and Western blotting, the α and β chains of Ia.2$^+$ and total class II have the same apparent molecular mass (5), meaning that Ia.2$^+$ and Ia.2$^-$ class II molecules are conformers, where some aspect of the conformational difference impacts the lipid raft partitioning and functional properties of the molecule.

In this study, we demonstrate that differential pairing of highly conserved transmembrane (TM) domain G*XXX*G dimerization motifs controls MHC class II conformer forma-

* This work was supported, in whole or in part, by National Institutes of Health Grants AI–083922 (to J. R. D. and J. A. H.), AI–065773 (to J. R. D.), and PO1 AI-056321 to the Center for Immunology and Microbial Disease.
[1] To whom correspondence should be addressed: Albany Medical College, Center for Immunology and Microbial Disease, 47 New Scotland Ave., MC-151, Albany, NY 12208. Tel.: 518-262-9337; Fax: 518-262-6161; E-mail: drakej@mail.amc.edu.

[2] The abbreviations used are: ER, endoplasmic reticulum; CIITA, class II transactivator; Ii, invariant chain; TM, transmembrane domain; Endo H, endoglycosidase H; CHI, CNS searching of helix interactions; Aαk, I-A^k α chain; Aβk, I-A^k β chain; PE, phycoerythrin.

tion and that class II conformer creation occurs in the ER of the cell. These findings provide a new level of understanding of MHC class II structure and its impact on class II-driven immune functions.

MATERIALS AND METHODS

Cell Culture—TA3 B cells and I-A^k-expressing K46μ B cells (1D6 A10) were grown in RPMI 1640 media containing 10% FBS, 50 μM 2-mercaptoethanol, 1× nonessential amino acids, 1× sodium pyruvate, and fresh L-glutamine as reported previously (1D6 A10 cell media also contained 650 μg/ml G418 and 1 mg/ml hygromycin B (5)). CIITA-expressing HEK293T cells (6) were grown in DMEM 10% FBS, 50 μM 2-mercaptoethanol, 1× nonessential amino acids, 1× sodium pyruvate, and fresh L-glutamine and L-histidinol.

Immunofluorescence Microscopy—1D6 A10 I-A^k-expressing B cells were attached to glass coverslips, fixed with periodate-lysine-paraformaldehyde (7), washed, and permeabilized/stained in the presence of 0.02% saponin. Staining antibodies were 11-5.2-Alexa Fluor 488 (BioLegend 110009) and 10-3.6-Alexa Fluor 647 (BioLegend 109912), anti-Ii (In-1, BD Pharmingen 555317) followed by Alexa Fluor 594 goat anti-rat IgG (H+L) (Molecular Probes A11007) or rabbit anti-calnexin (Santa Cruz Biotechnology Sc-1139) followed by Alexa Fluor 594 donkey anti-rabbit IgG (H+L) (Molecular Probes A21207). Samples were mounted in Fluoro-Gel II with DAPI (EMS 17985-50) and imaged on an Olympus IX81 inverted confocal microscope equipped with a FluoView FV1000 illumination system, using a 60× water immersion objective with an NA of 1.2. Confocal slices were 0.57 μm thick.

Endo H Treatment—Immunoprecipitates were resuspended in 250 μl of denaturation buffer (0.1% SDS, 50 mM 2-mercaptoethanol) and heated to 100 °C for 10 min. Aliquots were then treated for 3 h at 37 °C with increasing concentrations of endoglycosidase H (Endo H) and analyzed by SDS-PAGE and Western blot.

Transient Transfections—CIITA-expressing HEK293T cells were transfected with full-length I-A^k α chain cDNA (in pcDNA3.1(+)] and β chain cDNA [pcDNA3.1/Hygro(+)) as indicated using FuGENE-HD transfection reagent (Promega E2311). Cells were collected 24 h after transfection, stained with 10-3.6-PE (BioLegend 109908) and 11-5.2-FITC (BD Biosciences 553536) and analyzed by flow cytometry.

Analysis of Flow Cytometry Staining—Transfection of 293T cells results in a population of cells with a broad range of total I-A^k class II expression. However, in cells expressing wild type (WT) I-A^k, expression of the Ia.2$^+$ conformer is directly proportional to total class II expression (see Fig. 4, *A* and *B*). In cells expressing mutant I-A^k molecules that have decreased Ia.2 expression, the cells are "shifted to the left" on a dot plot of total *versus* Ia.2$^+$ class II (*i.e.* for a given level of *total* I-A^k (*y*-axis), they exhibit a decreased level of staining for Ia.2 (*x*-axis)). To quantitate these results across multiple experiments, we generated two regions on the dot plots of total I-A^k *versus* Ia.2 class II (see Fig. 4*B*). One region is tightly gated on cells expressing WT I-A^k. The second gate is to the left of the first gate and includes any cells with a less than WT level of Ia.2 staining. For each condition in each experiment, we determined the fraction of all class II-positive cells (cells in either gate) expressing a WT level of Ia.2 (*i.e.* that fall in the WT gate). These values were averaged across multiple experiments and subject to appropriate statistical analysis (see Fig. 4, *C* and *D*).

Stable Transfections—Stable I-A^k transfectants of K46μ B cells were generated using our published protocol (5).

Computational Searches Using CHI—Structural calculations were carried out using the CNS searching of helix interactions (CHI) method (8), on an eight-node dual 2.66-GHz Xenon processor Linux cluster (Streamline computing, Warwick, UK) as described previously (9). cis MHC class II $\alpha\beta$ heterodimer models (containing parallel helices with N and C termini on the same face) were calculated for the TM domain sequences ALGLSVGLVGIVVGTIFII (α-chain) and MLSGIGGCVLGVIFLGLGL (β chain) or their indicated mutants. Starting geometries incorporated both left-handed and right-handed crossing angles of 25°, with a distance of 10.4 Å between the helices. Full searches of the heterodimer were carried out by rotating each helix around its central axis through 360° in increments of 45° followed by simulated annealing and energy minimization. Clusters containing 10 or more structures with a backbone root mean squared deviation of $<$1 Å were created and an average structure calculated.

Lipid Raft Isolation—Lipid rafts were isolated from transfected K46μ B cells solubilized in ice-cold 0.1% TX-100 as reported previously (5). Class II molecules were immunoprecipitated from gradient fractions with 1.5 μg of 11-5.2 mAb and 10 μl of protein G-Sepharose. Blots were probed with an anti-class II β chain antibody as described previously (5).

RESULTS

Ia.2$^+$ Class II Forms in the Endoplasmic Reticulum—Our previous studies established the Ia.2 epitope as a marker of a lipid raft-tropic I-A^k MHC class II conformer that is able to drive B cell calcium signaling and enhanced antigen presentation to CD4 T cells (5, 11). In addition, we reported that Ii is associated with both total and Ia.2$^+$ class II (5). These Ii association results suggest that the Ia.2$^+$ class II conformer forms early in the class II biosynthetic pathway, but do not reveal the precise location of class II conformer formation, which is important to know because it will provide key insights into the mechanism of class II conformer creation and subsequent peptide loading.

To further investigate the location of class II conformer formation, we determined the Endo H sensitivity of the *N*-linked carbohydrate side chains (a characteristic of ER-resident proteins) of both total and Ia.2$^+$ class II. As shown in Fig. 1, a fraction of the α chains of both total and Ia.2$^+$ class II are Endo H-sensitive (*arrowhead*), consistent with formation of Ia.2$^+$ class II during the ER phase of the class II biosynthetic pathway.

To further define the location of formation of Ia.2$^+$ class II, I-A^k-expressing B cells were fixed, permeabilized, and stained with anti-Ia.2 and anti-total I-A^k mAbs (Fig. 2*A*). Consistent with the idea that Ia.2$^+$ class II forms early in the biosynthetic pathway, there is essentially complete overlap of the two staining patterns (Pearson's coefficient $>$0.9). The same B cells were also stained for either total or Ia.2$^+$ I-A^k class II and the ER marker calnexin or class II chaperone Ii, which is present early in the class II biosynthetic pathway (Fig. 2, *B–D*). Total and

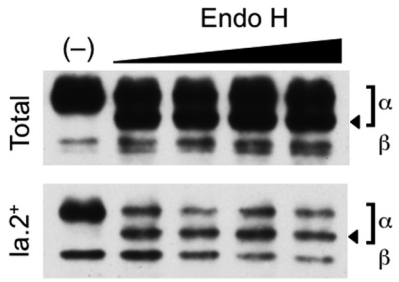

FIGURE 1. **Endoglycosidase H sensitivity of I-A^k class ii molecules.** B10.Br splenocytes were lysed, and either total or Ia.2$^+$ I-A^k class II molecules were immunoprecipitated with the 10-2.16 or 11-5.2 mAb, respectively. Samples were either left untreated (−) or treated with increasing amounts of Endo H. The samples were analyzed by SDS-PAGE and anti-class II antibody Western blotting. The positions of the class II α and β chains are indicated. The position of the Endo H digested α chain is indicated by an *arrowhead*. Surprisingly, the β chain of the Ia.2$^+$ class II conformer does not exhibit Endo H sensitivity, although the β chain of total class II does. Although we do not know the precise reason for this observation, one possibility could be that differences in the conformation or mechanism of formation of the Ia.2$^+$ class II molecule block β chain *N*-linked glycosylation. Shown are representative results from 1 of 4 independent experiments.

Ia.2$^+$ class II each exhibit the same degree of overlap with both intracellular markers. Although it is possible that Ia.2$^+$ class II conformers form after egress from the ER and are then delivered back to the ER via retrograde transport, the only reported incidence of class II retrograde transport back to the ER involves an N-terminal extended form of *human* invariant chain (which bears an ER retention motif), and that motif is only active when the cytoplasmic tails of class II are deleted (which is not the case in this system) (12). Therefore, the simplest interpretation of these findings is that Ia.2$^+$ class II conformers form in the ER, likely under the guidance of Ii.

A Role for Transmembrane GXXXG Dimerization Motifs in Formation of Ia.2$^+$ Class II—Early work by Cosson and Bonifacino (13) established a general role for I-A^k class II TM domain interactions involving highly conserved glycine residues in expression of the Ia.2 epitope, which at that time was thought to be present on *all* I-A^k class II molecules. However, we now know that the Ia.2 epitope marks a *subset* of

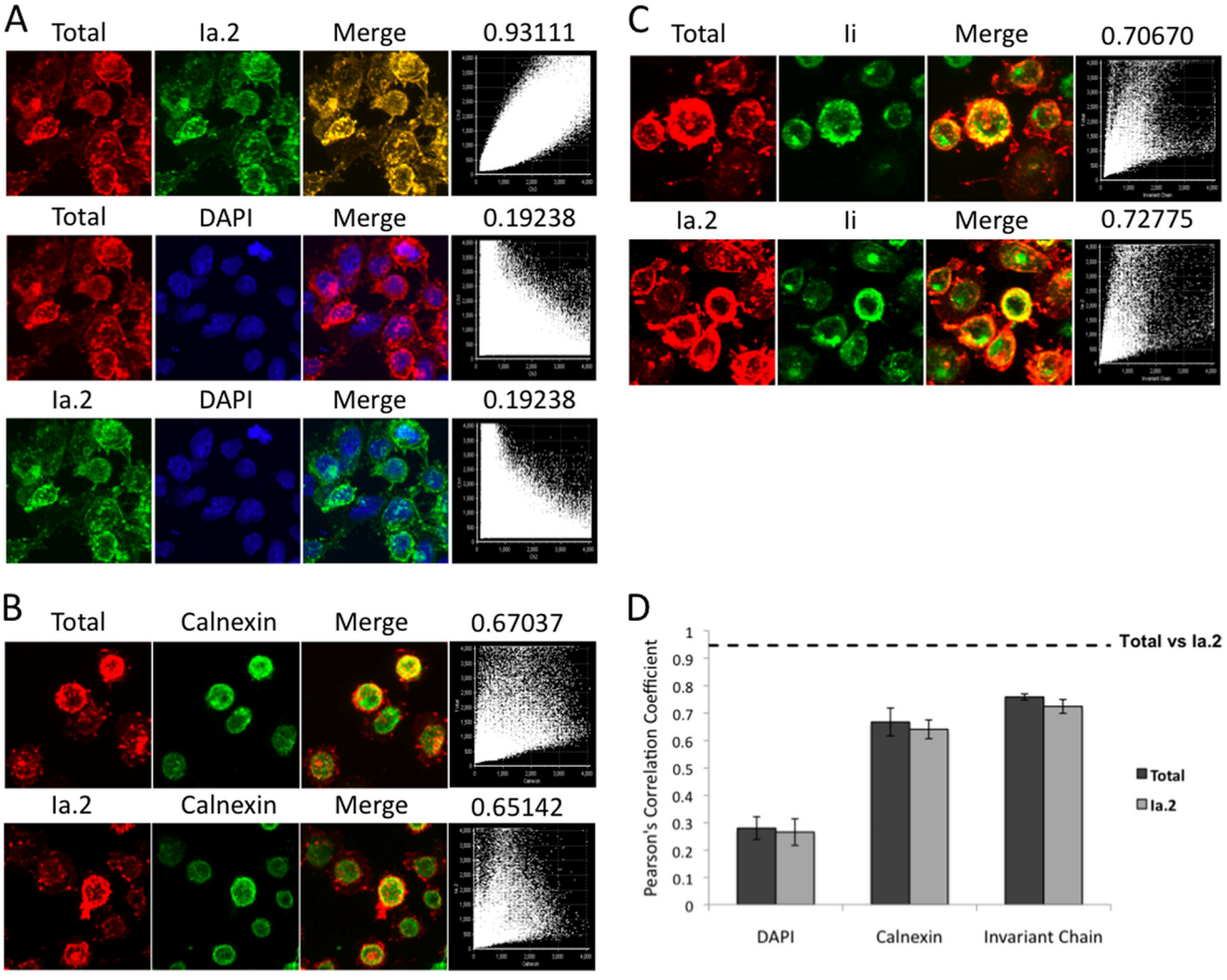

FIGURE 2. **Subcellular localization of Ia. 2$^+$ class II molecules.** *A*, I-A^k-expressing K46μ B cells were attached to coverslips, fixed, permeabilized with saponin, and stained with 11-5.2-(anti-Ia.2)-Alexa Fluor 488, 10-3.6-(anti-I-A^k)-Alexa Fluor 594, and DAPI. Shown are z-stack confocal images. Dot plots show the correlation of DAPI, Alexa Fluor 488, and Alexa Fluor 594 signal. The Pearson's correlation coefficient shown above each dot plot indicates the extent of marker correlation (1.00 equals 100% correlation). *B*, I-A^k-expressing B cells were stained for the ER marker calnexin and either total or Ia.2$^+$ class II and analyzed as in *panel A*. *C*, I-A^k-expressing B cells were stained for the class II chaperone Ii and either total or Ia.2$^+$ class II and analyzed as in *panel A*. *Panels A–C* show representative results from 1 of 3 or more independent experiments. *D*, plot of the average Pearson's correlation coefficient for 10 individual cell z-stacks analyzed and averaged for a total of three separate coverslips (30 total cells/condition). The *dotted line* indicates the Correlation Coefficient of total *versus* Ia.2$^+$ class II (*panel A*). The error bars indicate $\pm$ 1 S.D.

TABLE 1
Amino acid sequence of class II α and β chain transmembrane domains[1]

	M1[2] M2
I-A α-chain[3]	TVVCALGLSVGLVGIVVGTIFIIQGLRSGGTSRHPGPL
DQA[4]	TVVCALGLSVGLVGIVVGTVFIIQGLRSVGASRHQGPL
DRA[5]	NVVCALGLTVGLVGIIIGTIFIIKGVRKSNAAERRGPL
DPA[6]	TVLCALGLVLGLVGIIVGTVLIIKSLRSGHDPRAQGTL
I-E[f] α-chain[7]	NVVCALGLFVGLVGIVVGIILIMKGIKKRNVVERRQGAL
I-A β-chain[3]	KMLSGIGGCVLGVIFLGLGLFIRHRSQKGPRGPPPAGLLQ
DQB[8]	KMLSGVGGFVLGLIFLGLGLIIRQRSRKG LLH
DRB[9]	KMLSGVGGFVLGLLFLGAGLFIYFRNQKGHSGLQPTGFLS
DPB[10]	KTLTGAGGFVLGLIICGVGIFMHRRSKKVQRGSA
I-E[b] β-chain[11]	KMLSGVGGFVLGLLFLGAGLFIYFRNQKGQSGLQPTGLLS

1. Predicted transmembrane domains are underlined in I-A sequences.
2. Gray boxes — G*XXX*G motifs in I-A.
3. I-A consensus sequence based on seven I-A alleles (k, b, d, f, q, s, u).
4. DQA1*01:01:01 protein sequence from EMBL/EBI IMGT/HLA database.
5. All 7 DRA protein sequences from EMBL/EBI IMGT/HLA database.
6. All 10 DPA protein sequences from EMBL/EBI IMGT/HLA database.
7. NCBI Reference Sequence: NP_034511.2.
8. Consensus of most DQB protein sequences from EMBL/EBI IMGT/HLA database.
9. Consensus of most DRB protein sequences from EMBL/EBI IMGT/HLA database.
10. Consensus of most DPB protein sequences from EMBL/EBI IMGT/HLA database.
11. NCBI Reference Sequence: NP_034512.2.

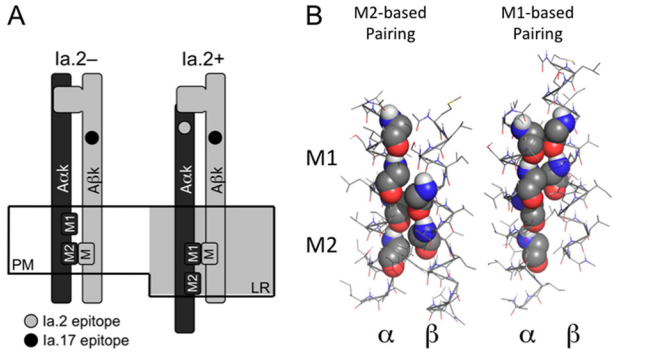

FIGURE 3. **Differential transmembrane domain G*XXX*G motif pairing and Ia. 2+ I-A^k class II molecules.** *A*, model of proposed G*XXX*G motif pairing of Ia.2$^+$ and Ia.2$^-$ I-A^k class II molecules at the plasma membrane (*PM*). In the non-raft-resident Ia.2$^-$ molecules, the β chain G*XXX*G motif pairs with the α chain C-terminal M2 motif (M2 conformer). In the lipid raft (*LR*)-resident Ia.2$^+$ molecules, the β chain G*XXX*G motif pairs with the α chain N-terminal M1 motif, supporting formation of a Ia.2$^+$ class II conformation (M1 conformer). *B*, interactions between the TM domains of the wild type murine I-A^k MHC class II molecule (Table 1) were modeled in CHI, and low energy solutions were obtained in which the β G*XXX*G chain motif paired with either the α chain M1 motif or the α chain M2 motif (motif residues are shown in *sphere representation*).

signaling-competent lipid raft-tropic I-A^k class II conformers (5). Moreover, our previous work established a general role for TM domain G*XXX*G dimerization motifs (originally identified and characterized in glycophorin (14)) in MHC class II α-β chain pairing (15).

Interestingly, G*XXX*G dimerization motifs usually function by pairing in a one-to-one manner, and whereas the class II β chain possesses one such motif, the α chain has two (Table 1). To investigate the potential role for differential pairing between TM domain G*XXX*G motifs in the formation of Ia.2$^+$ *versus* Ia.2$^-$ I-A^k class II conformers (Fig. 3*A*), we combined *in silico* molecular modeling of class II α-β chain TM domain interactions (15) with site-directed mutagenesis and analysis of Ia.2 epitope expression.

To allow us to combine the powerful immunological tools available to study murine I-A^k class II conformers with molecular modeling, we extended our prior computational modeling of human HLA class II TM domain interactions (where the computational analyses of helix-helix interactions were performed using the CHI program) to mouse class II TM domains (Fig. 3*B*). As shown in Table 1, the TM domains of mouse and human class II are highly similar, with human HLA-DQ being most closely related to mouse I-A. Consistent with the idea of a role for differential pairing of TM domain G*XXX*G dimerization motifs in driving formation of two distinct MHC class II conformers (Fig. 3*A*), computational modeling of mouse I-A TM domain interactions revealed two distinct low energy solutions, one in which the β chain G*XXX*G motif associates with the α chain N-terminal M1 G*XXX*G motif (M1 pairing) and a second with β packed against the α chain C-terminal M2 G*XXX*G motif (M2 pairing).

To test the hypothesis that the two modes of G*XXX*G motif pairing predicted by computational modeling correspond to the formation of the Ia.2$^+$ *versus* Ia.2$^-$ class II conformers, we turned to screening WT and mutant I-A^k molecules for Ia.2 expression using an established model system in CIITA-transfected HEK 293T cells. As reported previously (5), transfection of WT I-A^k class II α and β chains (*i.e.* Aαk and Aβk) into HEK293T cells leads to cells expressing Ia.2$^+$ I-A^k class II molecules (Fig. 4*A*). As a negative control, we expressed WT Aαk along with Aβk possessing a tethered peptide (Tether, which is known to ablate Ia.2 expression (5)) and obtained exclusive expression of Ia.2$^-$ I-A^k class II molecules. As predicted by the model presented in Fig. 3, mutation of the α chain N-terminal M1 G*XXX*G motif to A*XXX*A, V*XXX*V, or I*XXX*I (M1 G $\rightarrow$ A, M1 G $\rightarrow$ V or M1 G $\rightarrow$ I, respectively), which blocks motif pairing (16), results in a decrease in expression of the Ia.2$^+$ I-A^k class II conformer (Fig. 4*A*). Although this approach cannot establish the precise fraction of cell surface class II molecules in the Ia.2$^+$ conformer on the mutant cells, it is likely below 10–20% because our previous studies established this as the level of cell surface Ia.2$^+$ class II conformers on WT cells (5).

To quantify the impact of the M1 mutations on Ia.2 conformer expression, we used the gating strategy shown in Fig. 4*B* to determine the frequency of I-A^k class II-bearing cells that exhibit wild type *versus* decreased levels of the Ia.2 epitope expression (Fig. 4, *C* and *D*). Although the M1 G $\rightarrow$ A mutant (which is the most structurally conservative mutant) has only a slight impact on Ia.2$^+$ I-A^k conformer expression, both of the M1 G $\rightarrow$ V and G $\rightarrow$ I mutants exhibit a 50–60% reduction in Ia.2$^+$ I-A^k conformer expression. Although some of the M1 mutations do have a slight negative impact on *total* class II expression (possibly because they introduce bulky amino acid side chains into a region of the molecule where intimate chain paring is important for class II expression/surface stability), the impact of these mutations on Ia.2$^+$ conformer expression is significantly greater (see the legend of Fig. 4 for details).

Similar results were observed with K46μ B cells stably transfected with either WT or M1 G $\rightarrow$ A cDNA (in Fig. 4*E*, other constructs such as M1 G $\rightarrow$ V consistently yielded stable K46u transfectants, but these cells lacked strong overall I-A^k expression, suggesting that a more bulky residue at the M1 position is

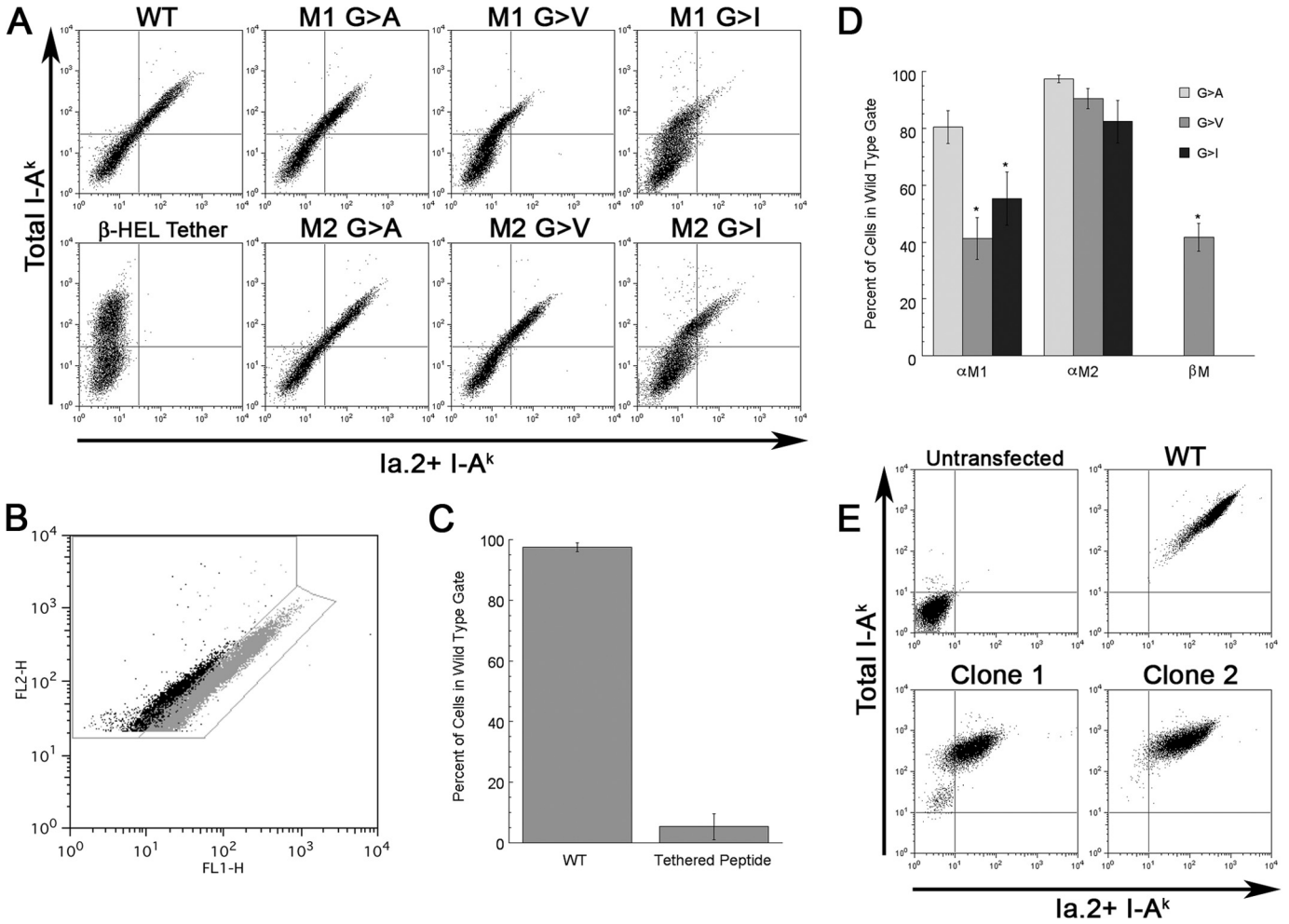

FIGURE 4. **Mutation of the I-A^k α chain M1 G*XXX*G motif results in selective diminution of Ia. 2+ class II expression.** *A*, CIITA-expressing 293T cells were transfected with the indicated I-A^k α (Aαk) and β (Aβk) chain cDNAs and cultured overnight to allow protein expression. Cells were stained with anti-Ia.2 (11-5.2-FITC) and anti-Ia.17 (10-3.6-PE) and analyzed by flow cytometry (gating on single live cells by forward scatter/side scatter and lack of propidium iodide staining). Shown is the Ia.2 *versus* Ia.17 expression for each $\alpha\beta$ chain pairing. Cells expressing WT I-A^k stain with both antibodies (*upper right quadrant of dot plot*). Cells expressing I-A^k with a tethered peptide (Aαk/Aβk-HEL) have essentially no Ia.2 staining as reported previously (5). Cells expressing α chain M1 mutations such as M1 G $\rightarrow$ V stain robustly for total class II (Ia.17) but exhibit decreased staining for Ia.2. Shown are representative results from one of greater than three independent experiments. *B*, gating strategy for quantification of Ia.2 epitope expression. The 11-5.2-FITC and 10-3.6-PE staining of viable class II-expressing 293T cells transfected with either WT (*gray*) or M1 G $\rightarrow$ V mutant (*black*) I-A^k class II is shown. Shown is the gate for WT Ia.2 expression as well as decreased Ia.2 expression. *C* and *D*, plots of frequency of I-A^k class II-positive transfected 293T cells that fall within the wild type gate (*panel B*). *Error bars* indicate $\pm$ 1 S.D. Reported are average values from 3–4 independent experiments. *E*, K46μ B cells were transfected with either WT I-A^k (WT Aαk + WT Aβk) or M1 G $\rightarrow$ A I-A^k (Aαk M1 G $\rightarrow$ A + WT Aβk) cDNAs, and stable transfectants were isolated and cloned (*Clone 1* and *Clone 2* are two representative clones). Cells were stained with 11-5.2-FITC and 10-3.6-PE and analyzed by flow cytometry (gating on single live cells by forward scatter/side scatter and lack of propidium iodide staining). Shown are representative results from 1 of 2 independent experiments where the same clones were stained with the 11-5.2 and 10-3.6 mAb. The two M1 G $\rightarrow$ A clones exhibit a 60% decrease in total I-A^k expression (*i.e.* they express 40% (41 and 39%) of the level of *total* class II as WT cells). If the M1 mutation had *no* effect on Ia.2$^+$ conformer formation, the cells would be expected to also express 60% of the Ia.2 epitope as WT. However, the M1 mutant cells express only about 9% (6.8 and 11.6%) the level of WT Ia.2 conformer, which is $\sim$75% less than would be expected.

detrimental to chain pairing and class II expression.). Although B cells transfected with M1 mutant I-A^k molecules express 50–60% less total I-A^k class II than cells transfected with WT I-A^k, M1 mutant transfected cells exhibit a >90% decrease in Ia.2 epitope expression (see the figure legend). These results indicate that the N-terminal α chain M1 G*XXX*G motif is critical for Ia.2$^+$ class II conformer formation, likely through its pairing with the single β chain motif (below).

Consistent with the proposed model (Fig. 3*A*) and expression results (Fig. 4), *in silico* computational analysis of the TM domain pairing of two of the α chain M1 mutants (*i.e.* M1 G $\rightarrow$ A and M1 G $\rightarrow$ V) revealed *no* low energy pairing solutions in which the β chain G*XXX*G motif paired with the mutated α chain M1 motif (Fig. 5). Moreover, in the M1 G $\rightarrow$ A and G $\rightarrow$ V mutants (where the small glycine side chain was replaced by an only slightly larger alanine or valine side chain), modeling predicts low energy solutions in which the β chain motif pairs with the *un*mutated α chain M2 motif. Therefore, the expression and molecular modeling results substantiate each other and are consistent with the model shown in Fig. 3*A*, in which β chain G*XXX*G motif pairing to the α chain N-terminal M1 G*XXX*G motif drives or supports formation of the Ia.2$^+$ M1 I-A^k class II conformer.

We next sought to further test the model presented in Fig. 3*A* by determining the impact of α chain M2 mutations on the formation of the Ia.2$^+$ class II conformer. If export of class II

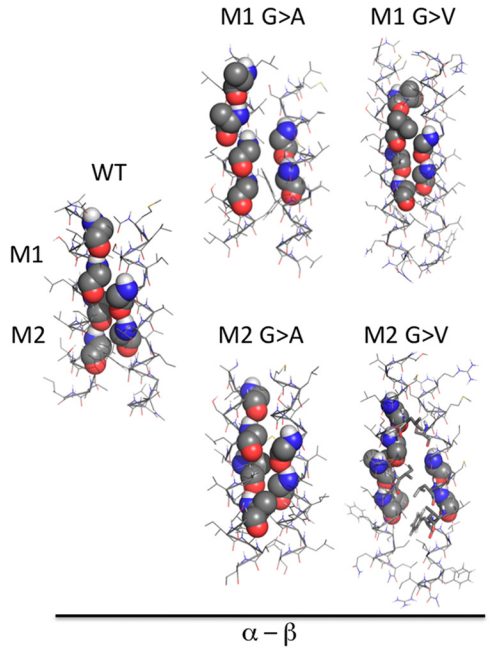

FIGURE 5. **Molecular modeling of I-A^k class II G*XXX*G motif mutants.** Interactions between the TM domains of the indicated murine I-A^k MHC class II α chains and wild type β chain were modeled in CHI. In the cases of the *M1* mutant class II molecules, *no* low energy solutions were obtained in which the β chain motif paired with the mutant α chain M1 motif (motifs and mutated motifs are shown as *spheres*). For M1 G → A and M1 G → V substitutions, one or more M2-like pairings solutions were obtained. The one low energy M2-based pairing observed with each mutant α chain that is most similar to that seen between wild type α and β is shown. The M2-based pairing observed with WT class II is shown for reference. In the case of the *M2* mutant class II α chain, *no* low energy solutions in which the β chain motif was paired with the *un*mutated α chain M1 motif were obtained. However, one or more M2-like pairings solutions were obtained. The one low energy M2-based pairing observed with each mutant α chain that is most similar to that seen between wild type α and β is shown.

molecules from the ER is absolutely dependent upon some form of α-β chain G*XXX*G motif pairing, then the model would predict enhanced Ia.2$^+$ M1 conformer formation with the Aαk M2 mutant (compared with WT), as this mutation would force α-β chain pairing via the unmutated N-terminal M1 motif (resulting in greater binding of the 11-5.2 anti-Ia.2 mAb). However, our previous work demonstrated that the α chain N-terminal M1 motif pairs weakly with the β chain motif (15), so if non-G*XXX*G motif paired class II molecules can exit the ER, the Aαk M2 mutant may not exhibit enhanced Ia.2$^+$ conformer formation.

As shown by the results presented in Fig. 4, *A* and *D*, mutation of the α chain M2 G*XXX*G motif to A*XXX*A, V*XXX*V, or I*XXX*I results in Ia.2 expression similar to (or slightly less than) wild type I-A^k class II (not enhanced expression of the Ia.2$^+$ conformer). This finding indicates that although the availability of the α chain M1 motif is necessary for formation of the Ia.2$^+$ I-A^k class II conformer (Figs. 4 and 5), the M1 motif on its own is not sufficient to drive Ia.2$^+$ conformer formation. This suggests that there may be other factors that limit use of the α chain M1 motif such as an accessory molecule that guides motif pairing (this possibility is discussed below).

We next turned to computational modeling of some of the Aαk M2 motif mutants (Fig. 5). As expected, none of the low energy solutions predict the β chain-forming quintessential G*XXX*G motif pairing with any of the mutant α chain M2 motifs (any M2-like pairing was unusual). However, for both analyzed mutants, we also obtained *no* low energy solutions in which the β chain motif paired with the *un*mutated α chain M1 motif. This was unexpected because each one of these mutants supports formation of the Ia.2$^+$ class II conformer (Fig. 4*A*). However, there is at least one potential explanation for this finding. Previous studies established that β chain pairing to the α chain M1 motif is significantly less robust than pairing to the M2 motif (15). Therefore, it is possible that the presence of two large side chain residues (*e.g.* valine) at the closely neighboring M2 motif may be sufficiently disruptive to prevent the modeling program from reaching a low energy M1-based pairing solution in isolation, although that pairing can form in the context of a lipid bilayer (possibly with the help of an accessory protein, see "Discussion"). These results would also suggest that although formation of the Ia.2$^-$ conformer aligns the TM domains in such a way as to allow $\alpha\beta$ pairing via the α chain M2 motif, formation of the Ia.2$^-$ conformer does not require this particular molecular pairing. Nevertheless, all of the data are consistent with the idea that formation of the Ia.2$^+$ M1 I-A^k MHC class II conformer is altogether dependent upon the presence of an unmutated α chain M1 motif to pair with the single β chain G*XXX*G motif.

Next, we turned our attention to the analysis of β chain G*XXX*G motif mutants. If formation of the Ia.2$^+$ class II conformer is driven by β chain motif pairing with the α chain M1 motif (Fig. 3), then ablation of the β chain motif should have an impact on Ia.2 expression similar to that of the α chain M1 motif mutants. To test this idea, we mutated the β chain G*XXX*G motif to V*XXX*V (βM G → V) and determined the impact on Ia.2 expression (Fig. 6). As predicted, mutation of the β chain motif (like mutation of the α chain M1 motif) decreases expression of the Ia.2+ class II conformer by over 50% (Figs. 4*D* and 6). In addition, computational modeling of the association between the mutated β chain TM domain and wild type α chain TM domain failed to reveal any low energy solutions in which the mutated β chain motif interacted with *either* the α chain M1 *or* the α chain M2 motif (Fig. 6*B*). Instead, mutation of the β chain G*XXX*G motif leads either to its exclusion from the heterodimer interface (Fig. 6*B*, *center panel*) or to packing against an alternate face of the α chain composed of Ser, Val, and Ile residues (Fig. 6*B*, *right panel*). Here again, impaired formation of the Ia.2$^+$ I-A^k class II conformer correlates with conditions that prevent G*XXX*G motif-based pairing between the α chain M1 motif and β chain motif.

Finally, we determined the lipid raft partitioning of WT and Aαk M1 G → A mutant class II molecules in stable K46μ B cell transfectants (Fig. 7). As reported previously (5), WT Ia.2$^+$ class II molecules are found almost exclusively in lipid rafts. In contrast, a large fraction of Aαk M1 G → A class II molecules are found outside of lipid rafts. Thus, the M1 G → A mutation that decreases formation of the Ia.2$^+$ class II conformer also impacts the biophysical/biochemical properties of the TM domain of the molecule to decrease lipid raft partitioning.

In total, the results presented in Figs. 3–7 reveal that formation of the Ia.2$^+$ lipid raft-tropic I-A^k class II conformer depends on pairing of the single β chain G*XXX*G dimerization

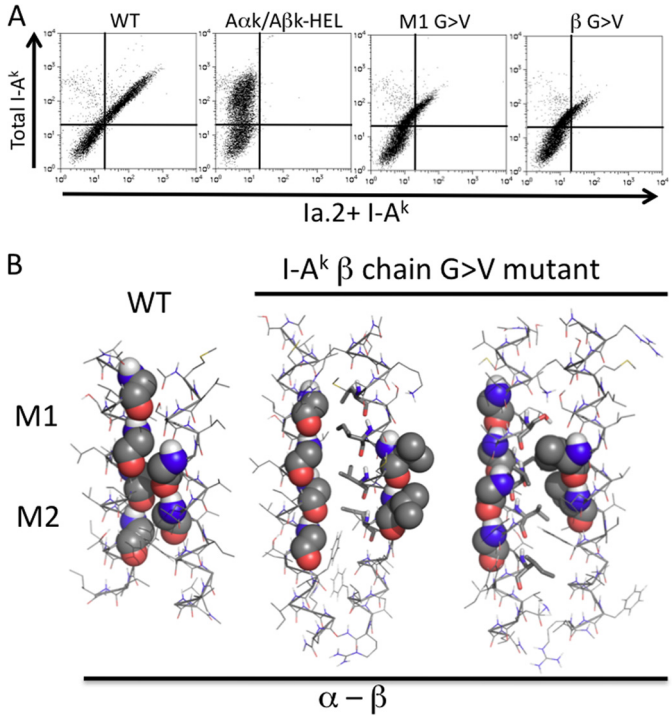

FIGURE 6. **Decreased Ia. 2+ class II expression by mutation of I-A^k β chain G*XXXG* motif.** *A*, CIITA-expressing 293T cells were transfected with the indicated I-A^k α (Aαk) and β (Aβk) chain cDNAs and Ia.2 *versus* Ia.17 expression determined as in Fig. 4. Shown are representative results from 1 of greater than 3 independent experiments. *B*, interactions between the TM domains of the murine I-A^k MHC class II β chain G $\rightarrow$ V mutant and wild type α chain were modeled in CHI. *No* low energy solutions in which the mutant β chain motif was paired with either the α chain M1 or the α chain M2 motifs were obtained. Instead, mutation of the β chain G*XXX*G led to exclusion of the motif from the heterodimer interface (*center panel*) in favor of use of an alternate face composed of hydrophobic residues (*stick representation*). Modeling runs also produced heterodimers in which the mutated β motif packs against an alternate face of the α chain composed of Ser, Val, and Ile residues (*right panel*). The M2-based pairing observed with WT class II is shown for reference.

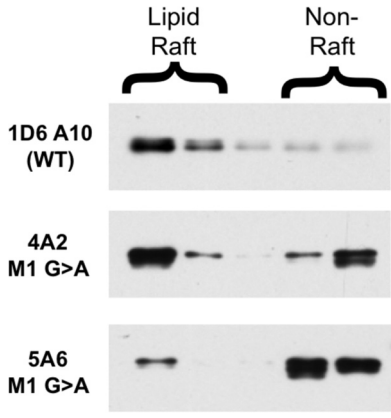

FIGURE 7. **Decreased lipid raft partitioning of α chain M1 mutant I-A^k class II molecules.** B cells expressing either WT or Aαk M1 G $\rightarrow$ A mutant I-Ak MHC class II molecules were solubilized in ice-cold 0.1% Triton X-100 to liberate lipid rafts (4A2 = Clone 1 from Fig. 4 and 5A6 = Clone 2). Lipid rafts were separated from non-raft material by sucrose density gradient centrifugation. I-A^k class II molecules were immunoprecipitated from each gradient fraction with the 11-5.2 mAb (which recognizes an epitope on the transfected Aαk chain, which is missing from the endogenous WT Aαd chain) and protein G-Sepharose. Immunoprecipitates were analyzed for class II molecules by Western blot with an anti-β chain antibody. Shown are representative results from 1 of 4 independent experiments (two in which class II was immunoprecipitated with 11-5.2 and detected by an anti-α chain Western blot (shown) and two in which 11-5.2-btn was bound to cell surface class II and detected by streptavidin Western blot (not shown)).

motif with the α chain N-terminal M1 G*XXX*G motif (the M1 conformer) and that formation of the Ia.2$^-$ non-raft-tropic conformer allows α-β chain pairing via the α chain C-terminal M2 (the M2 conformer).

DISCUSSION

Previous studies established the Ia.2 epitope as a marker of a subset of lipid raft-resident I-A^k class II molecules with unique signaling and antigen presentation capabilities (5, 11). Lipid raft-resident Ia.2$^+$ class II molecules drive Src family kinase-dependent calcium signaling in mature B cells and, consistent with the work of Roche and co-workers (17–19), are critically important for B cell antigen presentation and formation of B cell-T cell conjugates (5). Previous studies also suggested a role for TM domain G*XXX*G dimerization motifs in MHC class II α-β chain pairing (15). In this study, we provide a molecular explanation for the role of these motifs in determining MHC class II conformer formation by showing that differential pairing of the class II β chain G*XXX*G motif with one of two α chain motifs drives or enables formation of Ia.2$^+$ *versus* Ia.2$^-$ I-A^k class II conformers and controls the lipid raft partitioning properties of the molecule.

In a 1992 study by Cosson and Bonifacino (13) working in the same mouse I-A^k system, the authors demonstrated that wholesale mutation of *all* I-A^k TM domain glycine residues results in formation of an I-A^k class II conformer not recognized by the 11-5.2 anti-Ia.2 mAb. Here, we significantly extend and refine those findings by providing immunological and computational modeling evidence demonstrating that differential pairing of TM domain G*XXX*G dimerization motifs, originally identified and characterized in the erythrocyte TM glycoprotein glycophorin (14, 20), drives formation of Ia.2$^+$ *versus* Ia.2$^-$ class II conformers (Fig. 3).

Two questions naturally arise from the findings of this study. The first is the question of the mechanism controlling formation of the two distinct MHC class II conformers. The second is why antigen-presenting cells generate these two distinct class II conformers. Although we currently do not know the final answer to either question, we can offer some interesting insights.

As to the mechanism of formation of the two distinct class II conformers, the findings that the Ia.2$^+$ class II conformer associates with Ii (5) and is present in the ER (based on both Endo H sensitivity and colocalization with calnexin) suggest that both the Ia.2$^+$ and the Ia.2$^-$ class II conformer can be formed in the ER under the influence of Ii, which may act as a chaperone to guide conformer formation. This idea is consistent with our previous finding that the addition of a β chain tethered peptide (which would prevent/alter class II-Ii associations) blocks formation of Ia.2$^+$ class II (5) and with the work of Germain and co-workers (21), who demonstrated an interaction between the TM domains of Ii and class II, and suggest that the TM domain of Ii may interact with that of class II to guide G*XXX*G motif pairing. Studies are currently underway to investigate this intriguing possibility.

The model that initially drove these studies (Fig. 3) was based on the idea that pairing of the single β chain G*XXX*G motif with either α chain motif drives formation of one or the other class II

conformer. However, the finding that mutation of the α chain M2 motif does not result in increased formation of Ia.2$^+$ class II (by forcing only M1-based pairing) suggests that this model may be an oversimplification. However, there are two non-mutually exclusive potential refinements that would make the model consistent with all of the experimental findings. The first would be involvement of an accessory molecule that associates with the nascent class II molecule to catalyze/allow formation of Ia.2$^+$ class II. As discussed above, Ii is a likely candidate for this accessory molecule. On the other hand, one could consider the Ia.2$^+$ class II conformer a "stressed" form of the molecule that needs to be locked in place by β chain to α M1 pairing. In the absence of this pairing, the molecule "relaxes" to a less stressed Ia.2$^-$ form, which allows but does not require β chain to α M2 pairing. This second refinement is consistent with our finding that soluble forms of class II (which would lack a TM domain-based locking mechanism) adopt *only* the Ia.2$^-$ conformation.[3] The structure of the putative stressed Ia.2$^+$ form of class II is currently unclear, but preliminary comparisons of the various reported I-A^k crystal structures did reveal structural differences that might hold a clue. However, further analysis is necessary before making concrete conclusions.

As to the role of each class II conformer in the immune response, they almost certainly have two distinct functions. Intriguingly, *in vivo* imaging of lymph node B cell-T cell interactions revealed that in the absence of cognate antigen, B cells and T cells interact for a short period of time (*i.e.* <10 min), whereas after introduction of cognate antigen, those interactions can last for an hour or more (22). It is possible that these two types of B cell-T cell interactions are mediated by the two distinct class II conformers described in this study. Based on the potent B and T cell stimulation properties of the Ia.2$^+$ class II conformer (5, 11), it is most likely that antigen-derived peptides loaded onto Ia.2$^+$ class II molecules during B cell receptor-mediated antigen processing are responsible for the prolonged B cell-T cell interactions driven by cognate antigen. In contrast, Ia.2$^-$ peptide-class II complexes bearing self-peptides may drive the short term "homeostatic" interactions seen in the absence of cognate antigen. This scenario may even extend to other antigen-presenting cells such as dendritic cells and macrophages, where receptors for cognate antigen such as Fc receptors may have unique access to M1 conformer class II molecules (either functionally or physically), resulting in selective loading of foreign peptides onto these lipid raft-tropic class II molecules to drive efficient T cell activation. However, although seemingly likely, this speculation requires experimental confirmation.

Finally, MHC class II molecules are highly polymorphic, and many different human autoimmune diseases have been linked to the HLA class II locus. Although much work into the molecular mechanisms underlying this linkage has focused on the impact of allelic variations in the extracellular domain of the class II molecule, there are essentially no studies that focus on the role of the TM domain of the molecule. Interestingly, three autoimmunity-associated HLA-DQ α chains (*i.e.* DQA1*01:02, DQA1*01:04, and DQA1*03:01) have TM domain amino acid substitutions in or around the G*XXX*G motifs that may change α-β chain pairing and MHC class II molecular structure and/or function (Table 2). Studies are currently underway to determine the impact of these autoimmunity-associated mutations on G*XXX*G motif-driven class II structure and function.

TABLE 2
Amino acid sequence of the transmembrane and cytoplasmic domains of autoimmunity-associated HLA-DQ α chains

Allele	Transmembrane[1,2] / Cyto Domain Sequence	Autoimmune Associated
Murine I-A α chain	TVVCALGLSVGLVGIVVGTIFIIQGLRSGGTSRHPGPL	No
DQA1*01:01:01	TVVCALGLSVGLVGIVVGTVFIIQGLRSVGASRHQGPL	No
DQA1*01:02	----------M----------	Yes – (23,24)
DQA1*01:04:01:01	----T----------	Yes – (23)
DQA1*03:01/02/03	----------L--R----------	Yes – (23-25)
DQA1*05:07	----------C---------R----------	Unknown – (5)

1. Predicted transmembrane domains are underlined in I-Aα sequences.
2. Gray boxes — G*XXX*G motifs in I-A α.

Overall, this study further establishes the Ia.2+ I-A^k class II conformer as a class II subset with unique conformational and functional properties and defines the role of alternative pairing of TM domain G*XXX*G dimerization motifs in determining MHC class II structure and function. Future studies will address both the precise roles of each of these subsets in the immune response as well as their potential ties to human autoimmunity.

Acknowledgments—We thank Dr. Kathleen Busman-Sahay for helpful discussions, Dr. Michelle Lennartz for critical reading of the manuscript, and the Center for Immunology and Microbial Disease Immunology Core Facility for flow cytometry services.

REFERENCES

1. Cyster, J. G. (2010) B cell follicles and antigen encounters of the third kind. *Nat. Immunol.* **11,** 989–996
2. Germain, R. N., and Hendrix, L. R. (1991) MHC class II structure, occupancy and surface expression determined by post-endoplasmic reticulum antigen binding. *Nature* **353,** 134–139
3. Sadegh-Nasseri, S., Natarajan, S., Chou, C. L., Hartman, I. Z., Narayan, K., and Kim, A. (2010) Conformational heterogeneity of MHC class II induced upon binding to different peptides is a key regulator in antigen presentation and epitope selection. *Immunol. Res.* **47,** 56–64
4. Lovitch, S. B., and Unanue, E. R. (2005) Conformational isomers of a peptide-class II major histocompatibility complex. *Immunol. Rev.* **207,** 293–313
5. Busman-Sahay, K., Sargent, E., Harton, J. A., and Drake, J. R. (2011) The Ia.2 epitope defines a subset of lipid raft-resident MHC class II molecules crucial to effective antigen presentation. *J. Immunol.* **186,** 6710–6717
6. Porter, K. A., Kelley, L. N., Nekorchuk, M. D., Jones, J. H., Hahn, A. B., de Noronha, C. M., Harton, J. A., and Duus, K. M. (2010) CIITA enhances HIV-1 attachment to CD4$^+$ T cells leading to enhanced infection and cell depletion. *J. Immunol.* **185,** 6480–6488
7. Gondré-Lewis, T. A., Moquin, A. E., and Drake, J. R. (2001) Prolonged antigen persistence within nonterminal late endocytic compartments of antigen-specific B lymphocytes. *J. Immunol.* **166,** 6657–6664
8. Brünger, A. T., Adams, P. D., Clore, G. M., DeLano, W. L., Gros, P., Grosse-Kunstleve, R. W., Jiang, J. S., Kuszewski, J., Nilges, M., Pannu, N. S., Read, R. J., Rice, L. M., Simonson, T., and Warren, G. L. (1998) Crystallography & NMR system: A new software suite for macromolecular structure determination. *Acta Crystallogr. D Biol. Crystallogr.* **54,** 905–921
9. Jenei, Z. A., Borthwick, K., Zammit, V. A., and Dixon, A. M. (2009) Self-association of transmembrane domain 2 (TM2), but not TM1, in carnitine

[3] J. R. Drake, unpublished results.

palmitoyltransferase 1A: role of G*XXX*G(A) motifs. *J. Biol. Chem.* **284,** 6988–6997
10. Lee, K. W., Jung, Y. A., and Oh, D. H. (2006) Four novel human leukocyte antigen-DQA1 alleles identified in the Korean population. *Tissue Antigens* **68,** 167–172
11. Nashar, T. O., and Drake, J. R. (2006) Dynamics of MHC class II-activating signals in murine resting B cells. *J. Immunol.* **176,** 827–838
12. Khalil, H., Brunet, A., Saba, I., Terra, R., Sékaly, R. P., and Thibodeau, J. (2003) The MHC class II β chain cytoplasmic tail overcomes the invariant chain p35-encoded endoplasmic reticulum retention signal. *Int. Immunol.* **15,** 1249–1263
13. Cosson, P., and Bonifacino, J. S. (1992) Role of transmembrane domain interactions in the assembly of class II MHC molecules. *Science* **258,** 659–662
14. Brosig, B., and Langosch, D. (1998) The dimerization motif of the glycophorin A transmembrane segment in membranes: importance of glycine residues. *Protein Sci.* **7,** 1052–1056
15. King, G., and Dixon, A. M. (2010) Evidence for role of transmembrane helix-helix interactions in the assembly of the Class II major histocompatibility complex. *Mol. Biosyst.* **6,** 1650–1661
16. Morkowski, S., Raposo, G., Geuze, H. J., and Rudensky, A. Y. (1999) Peptide loading in the endoplasmic reticulum accelerates trafficking of peptide:MHC class II complexes in B cells. *J. Biomed. Sci.* **6,** 53–63
17. Anderson, H. A., Hiltbold, E. M., and Roche, P. A. (2000) Concentration of MHC class II molecules in lipid rafts facilitates antigen presentation. *Nat. Immunol.* **1,** 156–162
18. Hiltbold, E. M., Poloso, N. J., and Roche, P. A. (2003) MHC class II-peptide complexes and APC lipid rafts accumulate at the immunological synapse. *J. Immunol.* **170,** 1329–1338
19. Poloso, N. J., and Roche, P. A. (2004) Association of MHC class II-peptide complexes with plasma membrane lipid microdomains. *Curr. Opin. Immunol.* **16,** 103–107
20. Russ, W. P., and Engelman, D. M. (2000) The GxxxG motif: a framework for transmembrane helix-helix association. *J. Mol. Biol.* **296,** 911–919
21. Castellino, F., Han, R., and Germain, R. N. (2001) The transmembrane segment of invariant chain mediates binding to MHC class II molecules in a CLIP-independent manner. *Eur. J. Immunol.* **31,** 841–850
22. Okada, T., Miller, M. J., Parker, I., Krummel, M. F., Neighbors, M., Hartley, S. B., O'Garra, A., Cahalan, M. D., and Cyster, J. G. (2005) Antigen-engaged B cells undergo chemotaxis toward the T zone and form motile conjugates with helper T cells. *PLoS Biol.* **3,** e150
23. Deitiker, P. R., Oshima, M., Smith, R. G., Mosier, D., and Atassi, M. Z. (2011) Association with HLA DQ of early onset myasthenia gravis in Southeast Texas region of the United States. *Int J Immunogenet* **38,** 55–62
24. Saruhan-Direskeneli, G., Kiliç, A., Parman, Y., Serdaroğlu, P., and Deymeer, F. (2006) HLA-DQ polymorphism in Turkish patients with myasthenia gravis. *Hum. Immunol.* **67,** 352–358
25. Zhu, W. H., Lu, J. H., Lin, J., Xi, J. Y., Lu, J., Luo, S. S., Qiao, K., Xiao, B. G., Lu, C. Z., and Zhao, C. B. (2012) HLA-DQA1*03:02/DQB1*03:03:02 is strongly associated with susceptibility to childhood-onset ocular myasthenia gravis in Southern Han Chinese. *J. Neuroimmunol.* **247,** 81–85